Tryptophan Scanning Mutagenesis of the First Transmembrane Domain of the Innexin Shaking-B(Lethal)

Adam DePriest,[†] Pauline Phelan,[‡] and I. Martha Skerrett[†*]
[†]Biology Department, Buffalo State College, Buffalo, New York; and [‡]School of Biosciences, University of Kent, Canterbury, Kent, United Kingdom

ABSTRACT The channel proteins of gap junctions are encoded by two distinct gene families, connexins, which are exclusive to chordates, and innexins/pannexins, which are found throughout the animal kingdom. Although the relationship between the primary structure and function of the vertebrate connexins has been relatively well studied, there are, to our knowledge, no structure-function analyses of invertebrate innexins. In the first such study, we have used tryptophan scanning to probe the first transmembrane domain (M1) of the *Drosophila* innexin Shaking-B(Lethal), which is a component of rectifying electrical synapses in the Giant Fiber escape neural circuit. Tryptophan was substituted sequentially for 16 amino acids within M1 of Shaking-B(Lethal). Tryptophan insertion at every fourth residue (H27, T31, L35, and S39) disrupted gap junction function. The distribution of these sites is consistent with helical secondary structure and identifies the face of M1 involved in helix-helix interactions. Tryptophan substitution at several sites in M1 altered channel properties in a variety of ways. Changes in sensitivity to transjunctional voltage (Vj) were common and one mutation (S39W) induced sensitivity to transmembrane voltage (Vm). In addition, several mutations induced hemichannel activity. These changes are similar to those observed after substitutions within the transmembrane domains of connexins.

INTRODUCTION

The innexin family of proteins constitutes gap junctions in arthropods and other prechordate animals (1). Chordate gap junctions are composed primarily of proteins of the connexin family; a small number of distantly related innexins, referred to as pannexins, are present in chordates but appear to function predominantly as single-cell, rather than intercellular channels (2,3). Although very little is known about the structure of innexin-based junctions, connexin-based junctions are well characterized (4). Each channel is composed of two hemichannels also known as connexons. A connexon is formed when six connexin proteins oligomerize forming a central pore. Connexins have four transmembrane domains (M1–M4), cytoplasmic amino-termini and carboxyl termini (NT and CT) and two extracellular loops (E1 and E2) (5,6). Three-dimensional structures of connexin-based gap junction channels confirm the dodecameric nature of the connexin protein complex and a *a*-helical secondary structure for the membrane-spanning domains (Cx43 (7); Cx26 (8); Cx26 (9)).

Arthropod gap junctions appear similar to connexin-based junctions in electron micrographs (3) with a slightly wider gap observed in invertebrates (10–12). In both cases, intercellular channels form in dense plaques at sites where adjacent cell membranes are held within a few nanometers of one another. Innexins are predicted to have the same membrane topology as connexins including four membrane-spanning domains and two extracellular loops. The extracellular loops are longer in innexins than connexins, with two, rather than three, conserved cysteines per loop (1,13). In oocyte expression studies, innexin-based gap junctions form heterotypically as well as homotypically, display a range of sensitivities to voltage, and are gated by protons (14,15), all properties shared by their connexin-based counterparts.

The *shaking-B* gene of *Drosophila* was the first innexin shown to encode functional gap junction channels (16) and is one of the best characterized members of this family. The gene encodes three proteins, ShakB(N), ShakB(N+16), and ShakB(L) (13), and is required in the GFS. The fly GFS (17), like that in other arthropods such as crayfish (18,19), is a neural circuit responsible for a stereotypical escape response. Classical studies in the crayfish showed that fast transmission is achieved by rectifying electrical synapses between the lateral giant interneurons and giant motorneurons (18). More recent studies in *Drosophila* have established that GFS synapses are assembled from *shakB* gene products (20). In particular, ShakB(N+16) is required presynaptically in the Giant Fiber interneurons and ShakB(L) is expressed in the postsynaptic tergotrochanteral muscle motorneurons. These proteins assemble rectifying heterotypic gap junctions suggesting that such junctions are the molecular basis of rectification at arthropod giant synapses (14).

We selected ShakB(L), which reliably forms both homotypic and heterotypic junctions in heterologous systems (14,16), for initial structure-function analysis of innexins. The first transmembrane domain provides an interesting

Submitted June 8, 2011, and accepted for publication October 6, 2011.

*Correspondence: skerreim@buffalostate.edu

Abbreviations used: GFS, giant fiber system; Gj, junctional conductance; Ij, transjunctional current; M1, first transmembrane domain; ShakB(L), Shaking-B(Lethal); ShakB(N), Shaking-B(Neural); ShakB(N+16), Shaking-B(Neural+16); Vj, transjunctional voltage; Vm, transmembrane voltage; WT, wild-type.

Editor: Tzyh-Chang Hwang.

0006-3495/11/11/2408/9 $2.00

doi: 10.1016/j.bpj.2011.10.004

target based on studies of proteins that are related in sequence (pannexins) or function (connexins). M1 contributes to the pore of pannexin- and connexin-based channels (9,21), although in both cases the pore is complex and composed of multiple domains. In connexins, the pore lining is formed in part by the amino terminus that folds into the cytoplasmic mouth of the pore, interacting with the cytoplasmic end of M1. Additional contributions to the pore occur at the cytoplasmic end, where the second transmembrane helix extends beyond the bilayer, and in the extracellular region, where the first extracellular loop lines the pore (9). The conduction pathway of pannexin channels includes residues at the extracellular end of M1 and residues in the carboxyl terminus. In a study involving accessibility of substituted cysteines in Panx1, adjacent sites in M1 (e.g., residues 58C–62C) and in the carboxyl terminus (e.g., residues 413C–426C) were reactive. These patterns are inconsistent with helical secondary structure and suggest that pannexin-based channels have structural features that are distinctly different than their connexin-based counterparts (21). The complexity of channels formed by connexins and pannexins highlights the importance of confirming the helicity of M1 and identifying the extent of its interactions with other domains in structure-function analyses.

In many membrane proteins, helical secondary structure of transmembrane domains is reflected in a pattern of residues involved in interhelical interactions. A diverse set of methods reveals critical amino acids at approximately four-residue intervals in transmembrane helices. For instance, in one of the first studies specifically aimed at identifying interactions between transmembrane segments, dimerization of glycophorin A was disrupted by mutations induced at 3.9-residue intervals along the helix (22). In other proteins, sequence-specific interactions have been identified including a GxxxG or GxxxxxxG motif that places glycine at positions where helices interact (23), and a serine zipper motif that places serines at positions 7, 14, and 21 of one helix and 1, 8, and 15 of another (24). More recently, a consensus motif for interhelical associations in integrins identified a set of large and small interacting side chains located at four-residue intervals on associated helices (25).

Several mutagenic approaches have proved successful in studies of transmembrane domain interaction including alanine scanning (22), pairwise substitution (26), alanine insertion (27), and tryptophan scanning (28,29). When combined with functional analysis at the biochemical or biophysical level these provide information about the nature and importance of helix-helix interactions. Tryptophan scanning has become the most broadly applied mutagenic approach for analysis of interhelical interactions in membrane proteins with transport function. The approach was first applied to the MotB protein from *Escherichia coli* (30) and has since been applied to a number of membrane proteins including the acetylcholine receptor channel (29,31), potassium channels (32–34), GABA receptor channels (35), copper transporters (28), and hyperpolarization activated cyclic-nucleotide gated channels (36). In some of these studies tryptophan scanning has been specifically applied to provide insight into the secondary structure of transmembrane domains (33,37), engineer mutant membrane proteins with specific properties (38), and to compare the structure of similar transporters (28).

Tryptophan scanning was selected for this structure-function analysis of ShakB(L) to establish the secondary structure of M1 and to examine the extent of interactions between M1 and other domains. Tryptophan substitution at many sites altered channel properties, and we characterized several of the most interesting mutants.

MATERIALS AND METHODS

Preparation of tryptophan mutants and cRNA

Drosophila shaking-B(lethal) was cloned into pSPJC2L. Tryptophan mutants were created using the Quikchange or Quikchange Lightning mutagenesis kits (Agilent Technologies-Stratagene, Santa Clara, CA). Primers were designed using the QuikChange Primer Design Program (Agilent Technologies - Stratagene) and custom synthesized by Integrated DNA Technologies (Coralville, IA) in 25 nmole quantities with standard desalting. Mutations were confirmed by sequencing through the coding region (Roswell Park Cancer Institute DNA Sequencing Facility, Buffalo, NY). DNAs were linearized with XhoI and RNA prepared using a standard mMessage mMachine RNA kit (Applied Biosystems/Ambion, Austin, TX). RNA was purified with lithium chloride and quantified using gel electrophoresis and ethidium bromide staining through comparison to an RNA 250 control (Applied Biosystems/Ambion).

Expression and recording from oocytes

The technique of recording intercellular currents from paired *Xenopus* oocytes was carried out as described by Skerrett et al. (39). Oocytes were removed from ovulating *Xenopus laevis* females and the follicular layer partially removed with collagenase (Type 1A, Sigma-Aldrich, St. Louis, MO). The remaining follicular layer was removed using fine forceps before oocytes were preinjected with 0.5 ng of morpholino antisense oligonucleotide directed against *Xenopus* Cx38 (Gene Tools, Philomath, OR). Approximately 24 h after preinjection, oocytes were injected with 5 ng of cRNA. Injected oocytes were incubated at 18°C for 12–24 h and then stripped of their vitelline membranes and paired overnight in agar wells. Oocytes were cleaned and digested in Oocyte Ringers 2 (82.5 mM NaCl, 2 mM KCl, 1 mM $MgCl_2$, 5 mM HEPES, pH 7.4) and maintained in modified Barth's (MB) solution (88 mM NaCl, 1 mM KCl, 0.41 mM $CaCl_2$, 0.82 mM $MgSO_4$, 1 mM $MgCl_2$, 0.33 mM $Ca(NO_3)_2$, 20 mM HEPES, pH 7.4) for injection, pairing, and recording.

To assess junctional conductance (Gj), paired oocytes were clamped at −20 mV using two Geneclamp Amplifiers (Molecular Devices, Sunnyvale, CA). One cell was then pulsed to +80 mV and -120 mV eliciting a 2 s transjunctional current (Ij) in the partnered oocyte. Currents were measured at their maximal level, which occurred within the first 100 ms of the voltage pulse for WT channels and most mutants. Current was measured at the end of a 2 s voltage pulse for S39W, which induced currents that activated rather than inactivated upon application of Vj. For all mutants, a detailed characterization of junctional properties was obtained with a set of longer voltage steps applied in 10 mV increments to maximum Vjs of ± 100 mV.

For studies of sensitivity to Vm, paired oocytes were clamped at identical holding potentials ranging from -100 mV to +60 mV while a Vj was elicited as described previously. For studies of Vm sensitivity in single

oocytes, cells were impaled with their vitelline layers intact and voltage pulses were applied from a holding voltage of -40 mV. Oocytes were bathed in MB while data were acquired and analyzed using pClamp10 software (Molecular Devices, Sunnyvale, CA). In the initial screening of tryptophan mutants, each mutant was studied heterotypically in pairings with WT ShakB(L) to avoid additive effects of mutations on function. Pairings between WT-injected oocytes served as a positive control and provided the baseline conductance for each batch of cells. Pairings between WT-injected oocytes and oocytes injected only with antisense morpholino (oligo/ShakB(L)) served as a negative control. A set of experiments was considered only if pairings between WT and antisense-injected oocytes failed to induce measurable intercellular currents and pairings between WT resulted in averaged conductance above 25 μS. Such high conductance positive controls allowed us to differentiate nonfunctional mutants from those with reduced function. Furthermore, working with a saturating concentration of RNA (5 ng/oocyte, see Fig. 5 *B*) negated the effect of small variations in RNA quantification or injection on overall coupling levels.

Statistical analysis

To determine if tryptophan substitution significantly altered function, the conductance induced by each mutant was averaged. This average was then compared to the average conductance induced by WT ShakB(L) on the same day. A Student's *t*-test was applied to determine if the mean value differed significantly ($p < 0.05$) from that of WT.

RESULTS AND DISCUSSION

Properties of ShakB(L) junctions

ShakB(L) expressed reliably and robustly in oocytes. Example traces are shown in Fig. 1 *A* and the behavior is summarized in a conductance (Gj) versus voltage (Vj) relationship in Fig. 1 *B*. In response to voltage pulses between 0 and $\pm$80 mV, steady-state conductance was best fit by a one-state Boltzmann equation yielding the parameters Gmin = 0.422 $\pm$ 0.008 and $V_{1/2}$ = -38.5 $\pm$ 1 mV for relatively negative Vj and Gmin = 0.467 $\pm$ 0.007, $V_{1/2}$ = 41.3 $\pm$ 1 mV for relatively positive Vj (all values represent mean $\pm$ SD). Gmin represents the normalized minimum Gj, and $V_{1/2}$ represents the voltage at which conductance is halfway between its maximum and minimum values. The Gj versus Vj relationship deviated from a one-state Boltzmann equation at voltages beyond $\pm$60 mV. These points are represented by open squares on the Gj versus Vj plot and were excluded from analysis.

The behavior of ShakB(L) expressed in oocytes was similar to that reported previously at Vjs between $\pm$80 mV (14). Gating at higher Vjs has not previously been characterized. In our experiments, macroscopic gating events at $\pm$100 mV deviated from the Boltzmann fit and were excluded from analysis. Although the values of Gmin represent a macroscopic residual conductance state also observed in single channel recordings of well-characterized connexin- and innexin-based junctional channels (40,41), in some gap junction channels, additional slow gating transitions have been shown to gate channels to a fully closed state similar to that induced by chemical gating (41,42). Further characterization of ShakB(L) will be necessary to characterize gating at high Vj.

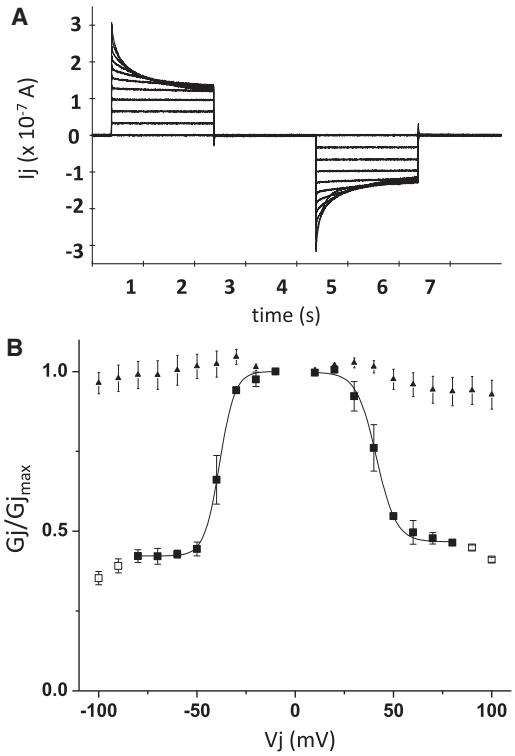

FIGURE 1 Characteristics of ShakB(L) gap junction channels between paired oocytes. (*A*) Intercellular currents recorded from paired *Xenopus* oocytes expressing ShakB(L). Paired oocytes were clamped at -20 mV. One oocyte was then pulsed to -120 mV and +80 mV in 10 mV steps while junctional currents were recorded from its partner. Outward currents represent current flowing out of the continuously clamped oocyte. (*B*) Average normalized conductance plotted as a function of voltage for three oocyte pairs expressing ShakB(L). Solid symbols represent steady-state conductance, open symbols represent instantaneous conductance for Vj between $\pm$80 mV. Steady-state conductance between 0 and -80 mV was fit by a one-state modified Boltzmann equation of the form Gj = (Gmax - Gmin)/[1 + exp(zF/RT(Vj - $V_{1/2}$)] yielding the parameters Gmin = 0.422 $\pm$ 0.008, $V_{1/2}$ = -38.5 $\pm$ 1 mV. Steady-state conductance between 0 and +80 mV was fit by a similar equation yielding the parameters Gmin = 0.467 $\pm$ 0.007, $V_{1/2}$ = 41.3 $\pm$ 1 mV. All parameters are presented as mean $\pm$ SD. At voltages beyond $\pm$80 mV conductance deviated from the one-state Boltzmann. These points are plotted (□) but were excluded from analysis.

Analysis of tryptophan substitutions in the M1

The first transmembrane domain of ShakB(L) was defined using the hydropathy analysis program TMHMM 2.0 (43). Residues S21-T43 are predicted to lie within the boundaries of the plasma membrane. We targeted 16 consecutive residues for tryptophan scanning beginning with F24, avoiding membrane boundaries where large aromatic side chains have the potential to influence positioning of helices within the membrane (44). Twelve of the 16 mutants induced junctional currents of at least normal magnitude while four were compromised in function. As shown in Fig. 2 *A*, the mutant H27W consistently failed to induce Gj, while T31W, L35W, and S39W were compromised in function. These residues

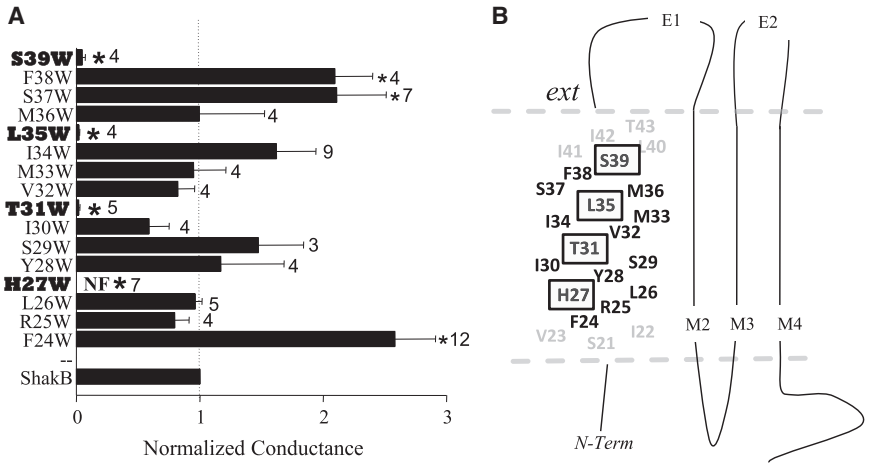

FIGURE 2 Summarized results of tryptophan insertion within the M1 of ShakB(L). (*A*) Bar chart summarizing the effect of tryptophan substitution on intercellular coupling at 16 sites within M1 of ShakB(L). Each result is normalized to the conductance of WT pairs in the same experiment. Mutants are arranged with the most extracellular sites on top. NF = nonfunctional, * = significantly different than WT at $p < 0.05$ as determined by a Student's *t*-test. Error bars represent mean ± SE. Numbers after each bar represent the number of oocyte pairs tested. (*B*) Predicted membrane topology of ShakB(L) with M1 displayed in helical net format. Tryptophan-sensitive sites are boxed, emphasizing their relative positions, which are consistent with helical secondary structure.

were arranged on a helical net plot to determine whether the results were consistent with helical secondary structure (Fig. 2 *B*).

Sensitivity to tryptophan insertion is consistent with helical secondary structure

When tryptophan-sensitive sites were plotted on a helical net diagram (Fig. 2 *B*) the sensitive sites formed a diagonal stripe spanning four rotations of a helix. Because a membranous environment favors hydrogen-bonded secondary structure, transmembrane domains are expected to assume helical or β-sheet secondary structure (45). The periodicity and specificity of the disruptions in ShakB(L) provides strong evidence that M1 is helical, rather than β-sheet, and identifies a face of the M1 helix that interacts with another domain.

Tryptophan mutants with interesting properties

Scanning mutagenesis often leads to identification of mutants with interesting properties. In some cases it may even be selected as a screening method for creation of mutants for further analysis (38). In this study, we identified ShakB(L) mutants that displayed a range of altered properties including altered sensitivity to Vj, altered sensitivity to Vm, and altered hemichannel gating. Each of these behavioral changes reflects disruption of a gating mechanism inherent to gap junction function.

Only one mutant, H27W, consistently failed to induce coupling in oocytes and we did not further assess the basis for disruption of function. Because packing of transmembrane helices plays an important role in folding of membrane proteins (in (45)) mutations along the interacting faces of transmembrane helices are likely to prevent proper localization. The histidine is highly conserved among *Drosophila* innexins (46). However, the preceding three residues are also highly conserved but tolerant to tryptophan substitution, including a conserved arginine at position 25 (Fig. 2 *A*).

Mutants with altered sensitivity to Vj

Mutants with altered sensitivity to Vj were most often observed when long sets of voltage pulses were applied to mutant-expressing oocytes. Most mutants displayed at least subtle changes in Vj sensitivity, reflected by asymmetry in the currents recorded from heterotypic pairings with WT ShakB(L). In our initial screening we did not record the orientation of currents with respect to the mutant-expressing oocyte and did not quantify the changes in gating behavior.

Fig. 3 shows current traces recorded from six different tryptophan mutants, all of which displayed changes in Vj sensitivity. The most radical change was observed with S39W, which activated rather than inactivated in response to Vj (Fig. 3 *A*). A mutant with very subtle changes in Vj sensitivity was M33W, which induced almost symmetric responses to Vj when paired with WT ShakB(L). Mutants such as F24W and F38W induced currents that inactivated asymmetrically, with inactivation occurring at lower voltages and to a greater extent than in homotypic WT ShakB(L) pairs (Fig. 3 *C*).

In total, we observed seven tryptophan mutants with obvious changes in Vj sensitivity. However, mutants that expressed robustly may have been overlooked because voltage sensitivity diminishes with increased conductance. Our observations regarding Vj-dependent gating tend to represent mutants with compromised function because these induced low levels of coupling with strong Vj sensitivity.

S39W displays altered sensitivity to Vj and Vm

When tryptophan was substituted for serine at position 39 (S39W), a reduction in Gj was accompanied by a reverse-gating phenotype (Fig. 3 *A*) observed previously in macroscopic recordings of connexin-based channels (47,48). The term "reverse-gating" refers to, and emphasizes, the tendency for currents to activate rather than inactivate in

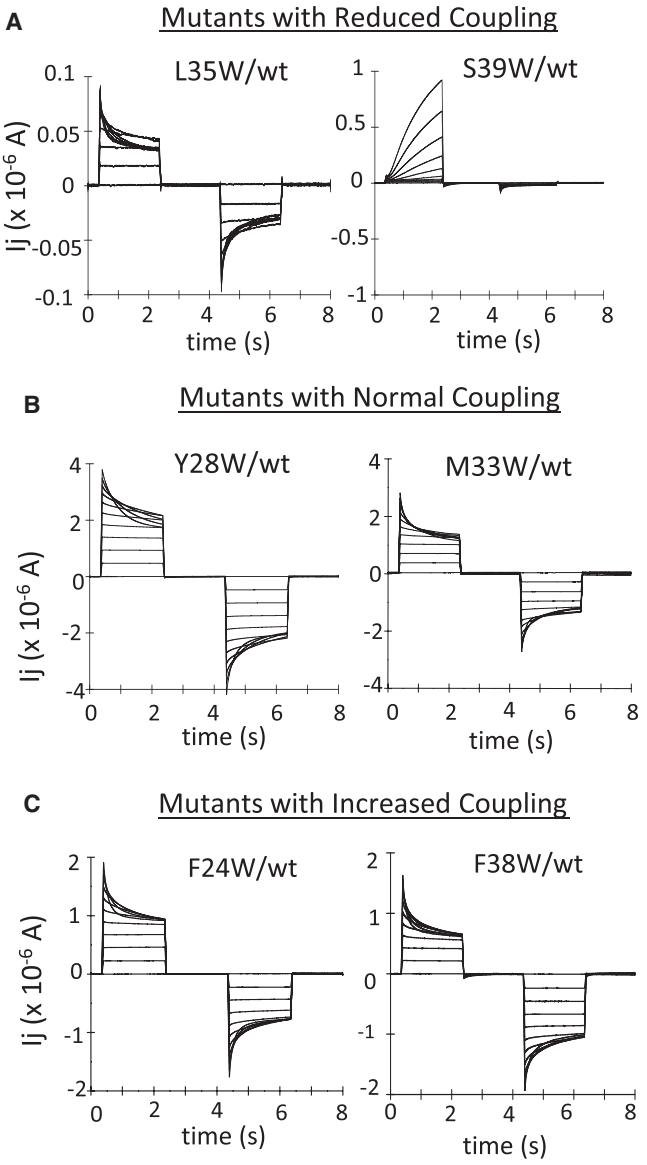

FIGURE 3 Intercellular currents recorded from paired *Xenopus* oocytes expressing tryptophan mutants showing the characteristics of gap junctions induced by mutants that (*A*) decreased intercellular conductance (L35W, S39W), (*B*) induced normal levels of conductance (Y28W, M33W), and (*C*) increased intercellular conductance (F24W, F38W). Coupling levels in the 20 μS range were established in the last group by injecting oocytes with about one-quarter the regular amount of RNA, to observe Vj-dependent gating. Paired oocytes were clamped at -20 mV and one oocyte was then pulsed to +80 mV and -120 mV in 10 mV steps while its partner was continuously clamped at -20 mV.

response to Vj. In studies of connexins, reverse-gating occurs in response to mutagenesis, particularly point mutations within the transmembrane domains (47,48). For instance, in Cx32, cysteine mutations in all four transmembrane domains induce reverse-gating and sensitive locations tend to be confined to a specific face of each helix (49). More detailed analysis of several of these sites suggested that amino acid side-chain properties such as length or branching are critical at specific locations. For example, in Cx32, replacing the methionine at position 34 with amino acids having shorter side chains (e.g., M34A, M34C, M34T, and M34S) induced reverse-gating; replacing M34 with leucine (M34L), an amino acid with a side chain comparable in length to that of methionine, had little effect on gating (48), while replacement with tryptophan (M34W) rendered the channels nonfunctional (49). These observations suggest that the reverse-gating phenotype correlates with disruption of interactions between helices in connexins. The changes observed after tryptophan substitution at S39 in ShakB(L) represent the first, to our knowledge, reported observation of reverse-gating in an innexin-based channel. The position of S39 on the interacting face of the M1 helix, along with H27, T31, and L35, suggests that disruption of helix-helix interactions can also induce reverse-gating of an innexin-based channel.

Gap junction channel properties were further assessed in ShakB(L)/S39W pairs by reversing the polarity of Vj. When this was done, the reverse-gating phenotype was maintained, however, the magnitude of the current differed. This suggested that the channels were sensitive to transmembrane holding potential (Vm) as well as Vj. A detailed analysis of Vm sensitivity was, therefore, carried out and the results are summarized in Fig. 4. When normalized to the Gj measured at -20 mV, S39W displayed steep sensitivity to Vm, decreasing greater than twofold at 20 mV and increasing by almost twofold at -60 mV. This is in contrast to WT ShakB(L), which is insensitive to Vm (16).

Analysis of ShakB(L)S39W represents the first report of a reverse-gating phenotype in an innexin-based junction, and suggests that a common mechanism may be disrupted by point mutations within the transmembrane domains of connexins and innexins. Plausibly, a disruption of interactions that stabilize the open state of the channel results in a partially closed conformation sensitive to the application of Vj. Because all channels with a reverse-gating phenotype tend to open in response to relatively positive Vjs (47,49,50) it is unlikely that disruption of a Vj gate is responsible for the phenomenon. In the case of S39W in ShakB(L), a high sensitivity to Vm occurred in addition to changes in Vj sensitivity. An altered hemichannel gating mechanism known as the loop gate (40,41) would have such an effect.

Three mutants induced large transmembrane currents in oocytes

Three tryptophan mutants (F24W, S37W, and F38W) induced higher Gj between paired oocytes than WT ShakB(L). These are denoted by asterisks on the bar graph in Fig. 2 *A* reflecting that the increase was statistically significant. The relative position of these residues within M1 is displayed on the helical net plot in Fig. 5 *A*. They are positioned close to the predicted cytoplasmic (F24)

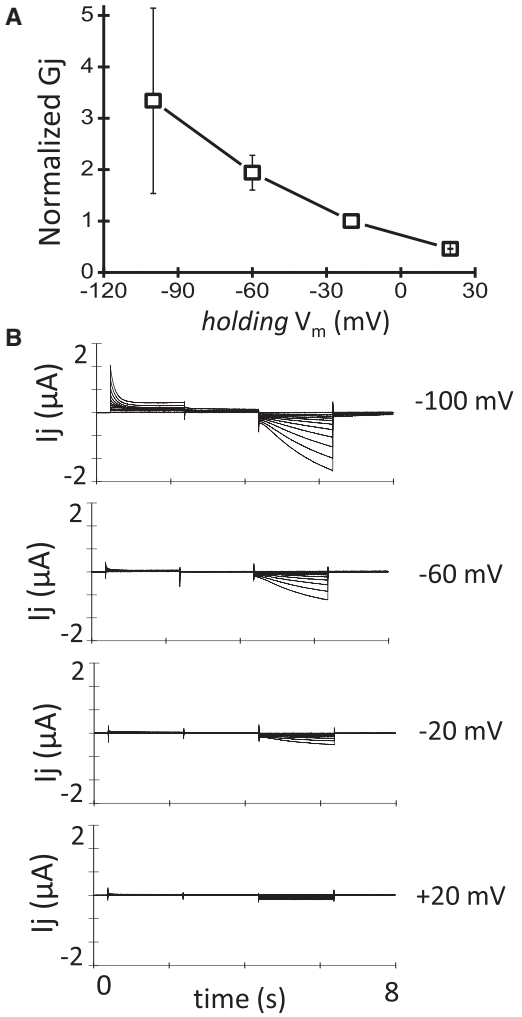

FIGURE 4 Tryptophan substitution at S39 creates ShakB(L) junctions that are sensitive to transmembrane holding potential (Vm). (*A*) Summary of changes in conductance as a function of Vm for WT/S39W junctions. Data were normalized to the conductance at Vm = -20 mV. Conductance was determined at different Vms by imposing a 2 s Vj pulse of 60 mV. Measuring transjunctional current at the end of this 2 s pulse allowed the activated state of the channels to be captured. Error bars represent mean ± SE. (*B*) Intercellular currents recorded from paired *Xenopus* oocytes expressing S39W and clamped at four Vms. All traces were recorded from the same heterotypic wt/S39W pair. Vj was induced by pulsing the WT-expressing oocyte to ±100 mV relative to the holding potential in 10 mV steps and current was always recorded from the S39W-expressing oocyte.

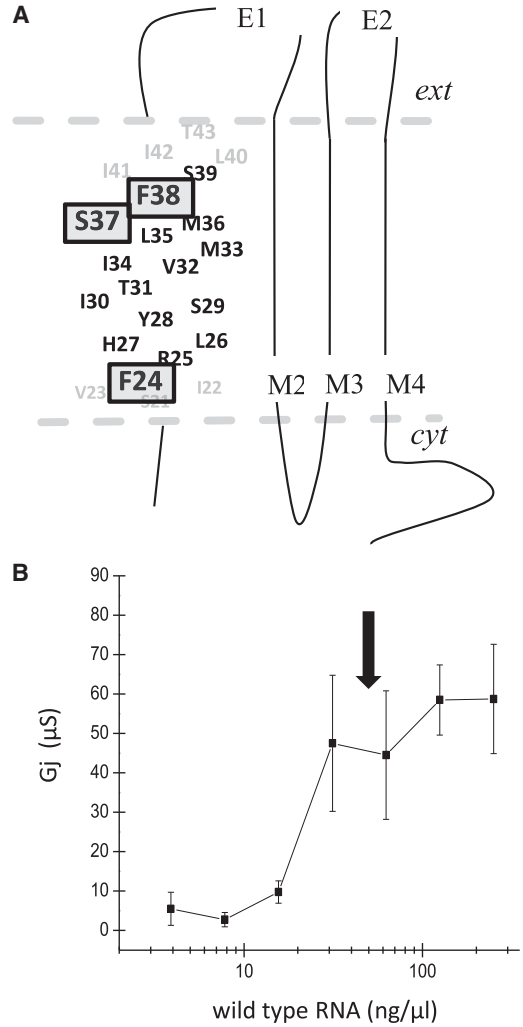

FIGURE 5 Three tryptophan substitutions in M1 caused an increase in Gj. (*A*) Topology plot of ShakB(L) highlighting sites where tryptophan substitution caused a significant increase in conductance. (*B*) Plot of RNA concentration versus conductance for WT ShakB(L) showing that saturating concentrations of RNA were used in the study. When comparing function of mutants, each oocyte was injected with 41 nl of RNA diluted to 125 ng/ml totaling 5 ng/oocyte (*black arrow*). Errors bars represent mean ± SE.

and extracellular (S37 and F38) borders of the M1 helix. Fig. 5 *B* shows that small variations in the RNA concentration cannot account for the large conductance increase induced by these mutants. The arrow in Fig. 5 *B* represents the RNA concentration used for analysis of tryptophan mutants.

After injection of RNA encoding the mutants F24W, S37W, and F38W the health of oocytes was compromised. However, once oocytes were paired for gap junction experiments survival rates increased. To test whether these mutations induced membrane currents in oocytes, voltage pulses were applied to study currents across the plasma membrane in the range -160 mV to +80 mV. For studies of membrane currents, oocytes were maintained in a solution of MB containing 0.74 mM Ca^{2+} and 1.82 mM Mg^{2+}. Attempts to transfer oocytes to typical solutions used for connexin hemichannel analysis, with extracellular calcium concentration at or <0.1 mM, caused the oocytes to swell and burst, prohibiting stable electrical recordings. Comparison of transmembrane currents induced by F24W, S37W, F38W, and WT ShakB(L) showed that expression of ShakB(L) does not induce transmembrane currents in oocytes, whereas all three tryptophan mutants induced large currents. As shown

in Fig. 6 *A*, the current versus voltage relationship for WT ShakB(L)-injected oocytes was similar to that of Cx38 antisense oligonucleotide-injected oocytes, whereas F38W induced large voltage-dependent currents. Fig. 6, *B* and *C*, show similar results for F24W and S37W, respectively, both of which induced large voltage-dependent membrane currents. Injecting oocytes with one-quarter the amount of RNA used in studies of paired oocytes induced smaller but significant currents across the plasma membrane. Because two of the sites (S37 and F38) are located at the extracellular end of M1, it is possible that tryptophan insertion induced hemichannel activity by disrupting interactions between the extracellular loops required to maintain the closed conformation of nonapposed channels (reviewed by (51).

Given the correlation between induction of membrane currents and high Gj mediated by F24W, S37W, and F38W one could speculate that the presence of open hemichannels induces junctional formation, a phenomenon previously observed when Cx46 and Cx50 were expressed in oocytes (52). All three mutants tended to maintain unusual sensitivity to Vj at high conductances. Wilders and Jongsma (53) suggested that junctions that maintain voltage sensitivity at higher conductance could be explained by the presence of a higher number of small junctions, analogous to a situation where several high resistors replace low resistance units in a circuit that involves significant contributions from electrode series resistance and cellular input resistance. We often observed sensitivity to Vj at conductances in the 100 μS range for these mutants, which is uncharacteristic of junctions formed by ShakB(L) or other junctional proteins expressed in oocytes. An example trace recorded from a 100 μS oocyte pair expressing S37W is shown in Fig. 6 *D*. Overall, the results suggest that increased hemichannel function tends to induce the rapid formation of many small junctional plaques.

CONCLUSIONS

Tryptophan scanning was used to establish the helical nature of the first transmembrane domain of the innexin ShakB(L). One face of the helix, including residues H27, T31, L35, and S39, was sensitive to tryptophan insertion, representing a localized region of contact between M1 and another transmembrane domain. Further experiments are required to determine whether the interacting face of M1 is involved in inter- or intrasubunit interactions.

Very little is known about the role of transmembrane domain interactions in gap junction channels. In innexins, as in other membrane proteins, transmembrane domain interactions are likely to stabilize tertiary structure, regulate protein function, and maintain quaternary structure by mediating subunit oligomerization (in (45)). We observed a range of effects when helical interactions were disrupted in ShakB(L). In the case of H27W, a complete disruption in function was observed, while T31W, L35W, and S39W induced very low levels of coupling. Further experiments are required to determine whether these mutations disrupt the efficiency of gap junction formation and/or impair the function of channels in otherwise normal plaques. Three

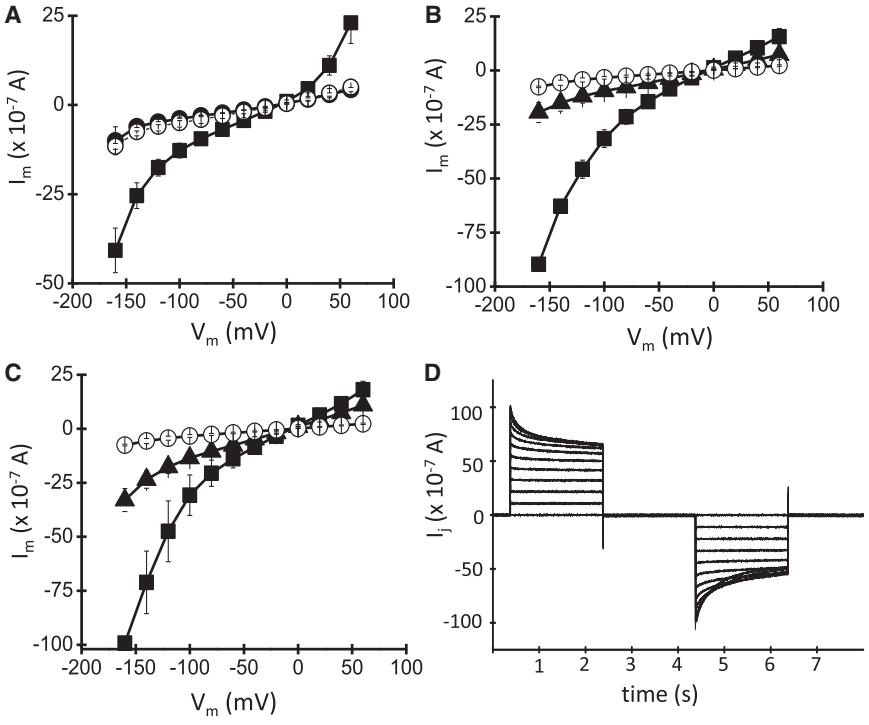

FIGURE 6 Three tryptophan mutants, F24W, S37W, and F38W, induced membrane currents in oocytes. (*A*) Current versus voltage plot summarizing currents across the plasma membrane (Im) of single oocytes injected with F38W RNA (■), WT RNA (●) or Cx38 antisense oligonucleotide (○). (*B*) Current versus voltage plot summarizing currents across the plasma membrane (Im) of single oocytes injected with F24W RNA (125 ng = ■; 32 ng = ▲) or Cx38 antisense oligonucleotide (○). (*C*) Current versus voltage plot summarizing currents across the plasma membrane (Im) of single oocytes injected with S37W RNA (125 ng = ■; 32 ng = ▲) or Cx38 antisense oligonucleotide (○). (*D*) Intercellular currents recorded from paired oocytes expressing S37W. Paired oocytes were clamped at -20 mV and currents were recorded from the continuously clamped oocyte, while its partner was pulsed to Vj of ±100 mV relative to the holding Vm in 10 mV steps. Error bars represent mean ± SE.

of the mutants with impaired function (T31W, L35W, and S39W) displayed changes in sensitivity to Vj, and S39W displayed sensitivity to Vm not previously reported in studies of ShakB(L). These observations suggest that disruption of helical interactions in innexins affects mechanisms regulating channel gating in response to Vm and Vj but does not preclude the possibility that mechanisms of channel formation are also disturbed.

Although innexins and connexins represent unrelated protein families, they perform similar functions by assembling into large plaques to mediate electrical and chemical coupling of adjacent cells. Correlations between structure and function are of particular interest in cases where unrelated proteins perform similar functions. Connexin and innexin proteins have a common membrane topology and are expected to oligomerize similarly to form intercellular channels. To our knowledge, there are currently no published results of tryptophan scanning for connexins but in the crystal structure of a gap junction channel composed of Cx26, the first transmembrane domain is packed between the N-terminus, which folds into the cytoplasmic mouth of the channel, and the fourth transmembrane domain that lies parallel and adjacent to it. M1 also interacts closely with M2 near the middle of the membrane where the helices cross one another (9). Our results appear to be inconsistent with a similar tight packing arrangement for M1 of the innexin ShakB(L), because this domain interacts along only one helical face.

Several ShakB(L) mutants with interesting phenotypes were generated as a byproduct of tryptophan scanning. The mutant S39W displayed a reverse-gating phenotype often observed after amino acid substitution within the transmembrane domains of connexin-based channels. In addition, several mutants displayed altered sensitivity to Vj, whereas F24W, S37W, and F38W induced currents across the plasma membrane of nonapposed oocytes. Similar changes are commonly observed after amino acid substitution within the transmembrane domains of connexins (4) and suggest that channels formed by innexins and connexins may have similar regulatory mechanisms.

In summary, our results confirm that M1 of the innexin ShakB(L) is helical and identify a localized region of contact between M1 and another transmembrane domain. Amino acid substitution within M1 of ShakB(L) induces similar changes to those observed after mutagenesis of connexins. Some of the mutants with interesting properties are likely to prove useful in future studies, particularly those aimed at characterization of the mechanisms underlying rectification at electrical synapses in the GFS of *Drosophila*.

REFERENCES

1. Phelan, P. 2005. Innexins: members of an evolutionarily conserved family of gap-junction proteins. *Biochim. Biophys. Acta.* 1711:225–245.
2. Dahl, G., and S. Locovei. 2006. Pannexin: to gap or not to gap, is that a question? *IUBMB Life.* 58:409–419.
3. Goodenough, D. A., and D. L. Paul. 2009. Gap junctions. *Cold Spring Harb. Perspect. Biol.* 1:a002576.
4. Harris, A. L. 2001. Emerging issues of connexin channels: biophysics fills the gap. *Q. Rev. Biophys.* 34:325–472.
5. Milks, L. C., N. M. Kumar, …, N. B. Gilula. 1988. Topology of the 32-kd liver gap junction protein determined by site-directed antibody localizations. *EMBO J.* 7:2967–2975.
6. Hertzberg, E. L., R. M. Disher, …, R. G. Cook. 1988. Topology of the Mr 27,000 liver gap junction protein. Cytoplasmic localization of amino- and carboxyl termini and a hydrophilic domain which is protease-hypersensitive. *J. Biol. Chem.* 263:19105–19111.
7. Unger, V. M., N. M. Kumar, …, M. Yeager. 1999. Three-dimensional structure of a recombinant gap junction membrane channel. *Science.* 283:1176–1180.
8. Oshima, A., K. Tani, …, G. E. Sosinsky. 2007. Three-dimensional structure of a human connexin26 gap junction channel reveals a plug in the vestibule. *Proc. Natl. Acad. Sci. USA.* 104:10034–10039.
9. Maeda, S., S. Nakagawa, …, T. Tsukihara. 2009. Structure of the connexin 26 gap junction channel at 3.5 A resolution. *Nature.* 458:597–602.
10. Leitch, B. 1992. Ultrastructure of electrical synapses: review. *Electron Microsc. Rev.* 5:311–339.
11. Shimohigashi, M., and I. A. Meinertzhagen. 1998. The *shaking B* gene in *Drosophila* regulates the number of gap junctions between photoreceptor terminals in the lamina. *J. Neurobiol.* 35:105–117.
12. Blagburn, J. M., H. Alexopoulos, …, J. P. Bacon. 1999. Null mutation in *shaking-B* eliminates electrical, but not chemical, synapses in the *Drosophila* giant fiber system: a structural study. *J. Comp. Neurol.* 404:449–458.
13. Phelan, P., and T. A. Starich. 2001. Innexins get into the gap. *Bioessays.* 23:388–396.
14. Phelan, P., L. A. Goulding, …, J. P. Bacon. 2008. Molecular mechanism of rectification at identified electrical synapses in the *Drosophila* giant fiber system. *Curr. Biol.* 18:1955–1960.
15. Starich, T. A., J. Xu, …, J. E. Shaw. 2009. Interactions between innexins UNC-7 and UNC-9 mediate electrical synapse specificity in the *Caenorhabditis elegans* locomotory nervous system. *Neural Dev.* 4:16–44.
16. Phelan, P., L. A. Stebbings, …, C. Ford. 1998. *Drosophila* Shaking-B protein forms gap junctions in paired *Xenopus* oocytes. *Nature.* 391:181–184.
17. Allen, M. J., T. A. Godenschwege, …, P. Phelan. 2006. Making an escape: development and function of the *Drosophila* giant fibre system. *Semin. Cell Dev. Biol.* 17:31–41.
18. Furshpan, E. J., and D. D. Potter. 1959. Transmission at the giant motor synapses of the crayfish. *J. Physiol.* 145:289–325.
19. Jaslove, S. W., and P. R. Brink. 1986. The mechanism of rectification at the electrotonic motor giant synapse of the crayfish. *Nature.* 323: 63–65.
20. Phelan, P., M. Nakagawa, …, J. P. Bacon. 1996. Mutations in *shaking-B* prevent electrical synapse formation in the *Drosophila* giant fiber system. *J. Neurosci.* 16:1101–1113.
21. Wang, J., and G. Dahl. 2010. SCAM analysis of Panx1 suggests a peculiar pore structure. *J. Gen. Physiol.* 136:515–527.
22. Lemmon, M. A., J. M. Flanagan, H. R. Treutlein, J. Zhang, and D. M. Engelman. 1992. Sequence specificity in the dimerization of transmembrane alpha-helices. *Biochemistry.* 31:12719–12725.
23. Russ, W. P., and D. M. Engelman. 2000. The GxxxG motif: a framework for transmembrane helix-helix association. *J. Mol. Biol.* 296:911–919.
24. Adamian, L., and J. Liang. 2002. Interhelical hydrogen bonds and spatial motifs in membrane proteins: polar clamps and serine zippers. *Proteins.* 47:209–218.

25. Berger, B. W., D. W. Kulp, …, W. F. DeGrado. 2010. Consensus motif for integrin transmembrane helix association. *Proc. Natl. Acad. Sci. USA.* 107:703–708.

26. Bosch, L., E. Ramon, …, P. Garriga. 2003. Structural and functional role of helices I and II in rhodopsin. A novel interplay evidenced by mutations at Gly-51 and Gly-89 in the transmembrane domain. *J. Biol. Chem.* 278:20203–20209.

27. Braun, P., B. Persson, …, G. von Heijne. 1997. Alanine insertion scanning mutagenesis of lactose permease transmembrane helices. *J. Biol. Chem.* 272:29566–29571.

28. De Feo, C. J., S. Mootien, and V. M. Unger. 2010. Tryptophan scanning analysis of the membrane domain of CTR-copper transporters. *J. Membr. Biol.* 234:113–123.

29. Guzmán, G. R., J. Santiago, …, J. A. Lasalde-Dominicci. 2003. Tryptophan scanning mutagenesis in the alphaM3 transmembrane domain of the *Torpedo californica* acetylcholine receptor: functional and structural implications. *Biochemistry.* 42:12243–12250.

30. Sharp, L. L., J. Zhou, and D. F. Blair. 1995. Tryptophan-scanning mutagenesis of MotB, an integral membrane protein essential for flagellar rotation in *Escherichia coli*. *Biochemistry.* 34:9166–9171.

31. Díaz-De León, R., J. D. Otero-Cruz, …, J. A. Lasalde-Dominicci. 2008. Tryptophan scanning of the acetylcholine receptor's betaM4 transmembrane domain: decoding allosteric linkage at the lipid-protein interface with ion-channel gating. *Channels (Austin).* 2:439–448.

32. Choe, S., C. F. Stevens, and J. M. Sullivan. 1995. Three distinct structural environments of a transmembrane domain in the inwardly rectifying potassium channel ROMK1 defined by perturbation. *Proc. Natl. Acad. Sci. USA.* 92:12046–12049.

33. Monks, S. A., D. J. Needleman, and C. Miller. 1999. Helical structure and packing orientation of the S2 segment in the Shaker K^+ channel. *J. Gen. Physiol.* 113:415–423.

34. Labro, A. J., I. R. Boulet, …, D. J. Snyders. 2011. The S4-S5 linker of KCNQ1 channels forms a structural scaffold with the S6 segment controlling gate closure. *J. Biol. Chem.* 286:717–725.

35. Ueno, S., A. Lin, …, N. L. Harrison. 2000. Tryptophan scanning mutagenesis in TM2 of the $GABA(_A)$ receptor *a* subunit: effects on channel gating and regulation by ethanol. *Br. J. Pharmacol.* 131:296–302.

36. Ishii, T. M., N. Nakashima, and H. Ohmori. 2007. Tryptophan-scanning mutagenesis in the S1 domain of mammalian HCN channel reveals residues critical for voltage-gated activation. *J. Physiol.* 579:291–301.

37. Hong, K. H., and C. Miller. 2000. The lipid-protein interface of a *Shaker* $K(^+)$ channel. *J. Gen. Physiol.* 115:51–58.

38. Irizarry, S. N., E. Kutluay, …, L. Heginbotham. 2002. Opening the KcsA K^+ channel: tryptophan scanning and complementation analysis lead to mutants with altered gating. *Biochemistry.* 41:13653–13662.

39. Skerrett, I. M., M. Merritt, …, B. J. Nicholson. 2001. Applying the *Xenopus* oocyte expression system to the analysis of gap junction proteins. *In* Methods in Molecular Biology: Connexin Methods and Protocols. R. Bruzzone and C. Giaume, editors. Humana Press, NJ. 225–249.

40. Bukauskas, F. F., and R. Weingart. 1993. Multiple conductance states of newly formed single gap junction channels between insect cells. *Pflugers Arch.* 423:152–154.

41. Bukauskas, F. F., and V. K. Verselis. 2004. Gap junction channel gating. *Biochim. Biophys. Acta.* 1662:42–60.

42. Banach, K., and R. Weingart. 2000. Voltage gating of Cx43 gap junction channels involves fast and slow current transitions. *Pflugers Arch.* 439:248–250.

43. Krogh, A., B. Larsson, …, E. L. Sonnhammer. 2001. Predicting transmembrane protein topology with a hidden Markov model: application to complete genomes. *J. Mol. Biol.* 305:567–580.

44. Mall, S. R., R. Broadbridge, …, J. M. East. 2000. Effects of aromatic residues at the ends of transmembrane α-helices on helix interactions with lipid bilayers. *Biochemistry.* 39:2071–2078.

45. Luckey, M. 2008. Membrane Structural Biology. Cambridge University Press, NY.

46. Stebbings, L. A., M. G. Todman, …, J. A. Davies. 2002. Gap junctions in *Drosophila:* developmental expression of the entire innexin gene family. *Mech. Dev.* 113:197–205.

47. Oh, S., Y. Ri, …, T. A. Bargiello. 1997. Changes in permeability caused by connexin 32 mutations underlie X-linked Charcot-Marie-Tooth disease. *Neuron.* 19:927–938.

48. Skerrett, I. M., J. F. Smith, and B. J. Nicholson. 1999. Mechanistic differences between chemical and electrical gating of gap junctions. *In* Current Topics in Membranes, *Vol. 49*. C. Peracchia, editor. Academic Press, CA. 249–269.

49. Toloue, M. M., Y. Woolwine, …, I. M. Skerrett. 2008. Site-directed mutagenesis reveals putative regions of protein interaction within the transmembrane domains of connexins. *Cell Commun. Adhes.* 15: 95–105.

50. Skerrett, I. M., J. Aronowitz, …, B. J. Nicholson. 2002. Identification of amino acid residues lining the pore of a gap junction channel. *J. Cell Biol.* 159:349–360.

51. Dahl, G. 1996. Where are the gates in gap junction channels? *Clin. Exp. Pharmacol. Physiol.* 23:1047–1052.

52. Beahm, D. L., and J. E. Hall. 2004. Opening hemichannels in nonjunctional membrane stimulates gap junction formation. *Biophys. J.* 86: 781–796.

53. Wilders, R., and H. J. Jongsma. 1992. Limitations of the dual voltage clamp method in assaying conductance and kinetics of gap junction channels. *Biophys. J.* 63:942–953.